heritage

MDPI

Article

A Study on the Degradation of Iron Gall Inks and to Preserve Them Using Green Approaches

Natércia Teixeira [1,†], Paula Nabais [2,†], Vanessa Otero [2,3], Rafael Javier Díaz Hidalgo [4], Matteo Ferretti [5,†], Maurizio Licchelli [5] and Maria J. Melo [2,6,*]

1 LAQV-REQUIMTE, DQB, Faculty of Sciences, Universidade do Porto, Rua do Campo Alegre, s/n, 4169-007 Porto, Portugal; natercia.teixeira@fc.up.pt
2 LAQV-REQUIMTE and DCR, Nova School of Science and Technology, 2829-516 Caparica, Portugal; p.nabais@fct.unl.pt (P.N.); van_otero@fct.unl.pt (V.O.)
3 VICARTE, Department of Conservation and Restoration, NOVA School of Science and Technology, Nova University of Lisbon, Campus da Caparica, 2829-516 Caparica, Portugal
4 Departamento de Historia, Facultad de Filosofía y Letras, Universidad de Córdoba, Pl. Cardenal Salazar, 14003 Córdoba, Spain; l72dihir@uco.es
5 Department of Chemistry, University of Pavia, Via Taramelli 12, 27100 Pavia, Italy; matteo.ferretti02@universitadipavia.it (M.F.); mali@unipv.it (M.L.)
6 Institute of Medieval Studies (IEM), NOVA University of Lisbon, Av. Prof. Gama Pinto, 1646-003 Lisboa, Portugal
* Correspondence: mjm@fct.unl.pt
† These authors contributed equally to this work.

Abstract

Inks from the 12th to the 17th century were aged, and a multi-analytical approach was used for their identification based on HPLC–DAD–MS, microFTIR, and microRaman. Colorimetry analysis was also performed. After 6 years of application on filter paper, three inks were selected to be cleaned using a novel green approach based on a chemically crosslinked gel to remove unwanted materials from the ink surface. A Braga ink produced in 2018 was also tested. Two degradation products were identified; iron sulfate was the main degradation product in the Braga ink. For Montpellier, Guadalupe, and QI.8 inks, the main degradation product was a complex of iron with ellagic acid. These compounds were accurately confirmed using microFTIR. Several tests were performed to clean these degradation products with the gels. The Braga ink was cleaned with 10% ethanol in water, which was included in the gel, and the iron sulfate was removed within 15 s of application. On the other hand, the complex of iron with ellagic acid demanded longer application times; we used 2 min and repeated the application until the compound was removed. The novelty of this research has practical implications for the conservation of historical documents and artworks.

Keywords: iron gall inks; green approach; conservation; cultural heritage

Academic Editors: Cristina Cicero, Monia Vadrucci and Silvia Bottura Scardina

Received: 27 May 2025
Revised: 18 June 2025
Accepted: 23 June 2025
Published: 3 July 2025

Citation: Teixeira, N.; Nabais, P.; Otero, V.; Díaz Hidalgo, R.J.; Ferretti, M.; Licchelli, M.; Melo, M.J. A Study on the Degradation of Iron Gall Inks and to Preserve Them Using Green Approaches. *Heritage* **2025**, *8*, 261. https:// doi.org/10.3390/heritage8070261

1. Introduction

1.1. Relevance of Iron-Gall Inks

The urgency of preserving iron gall inks in cultural heritage is crucial [1–8]. Iron gall inks were typically prepared by combining plant extracts, such as those from *Quercus infectoria*, with iron salts and gum arabic [1,2,5,6]. The ink is perceived as black and is based on Fe^{3+}-complexes with phenolic compounds [5–7]. However, this black color transforms into shades of brown over time, a phenomenon that remains largely unexplained [1,9].

Gallic acid, until very recently, was considered the main component of gallnut extracts, and consequently, iron gallate complexes were considered the main chromophores of iron gall inks. However, crucial research has shown that there is more to be understood about these inks [10–13]. Through the use of historically accurate reconstructions of Iberian inks and a multi-analytical approach, Melo and Teixeira et al. have demonstrated that different manufacturing processes result in distinct iron gall ink compositions. They showed that the main components present can also be galloyl esters of glucose, such as pentagalloylglucose (PGG) and hexagalloylglucose (HGG) [5,12,13], as shown in Figure 1. This not only agrees with the results on Fe^{3+} coordination obtained by Lerf and Wagner using Mössbauer spectroscopy [14,15] but also has significant implications for our understanding of ink composition. These authors demonstrated that Fe^{3+}-gallate complexes, which bind through the carboxylate group, cannot form at the pH range found in ink preparation, which is between 2 and 3. They indicate that iron oxyhydroxides best represent the iron clusters and that these nanoparticles are "covered by a shell of polymerized oxidation products of the phenols" [15].

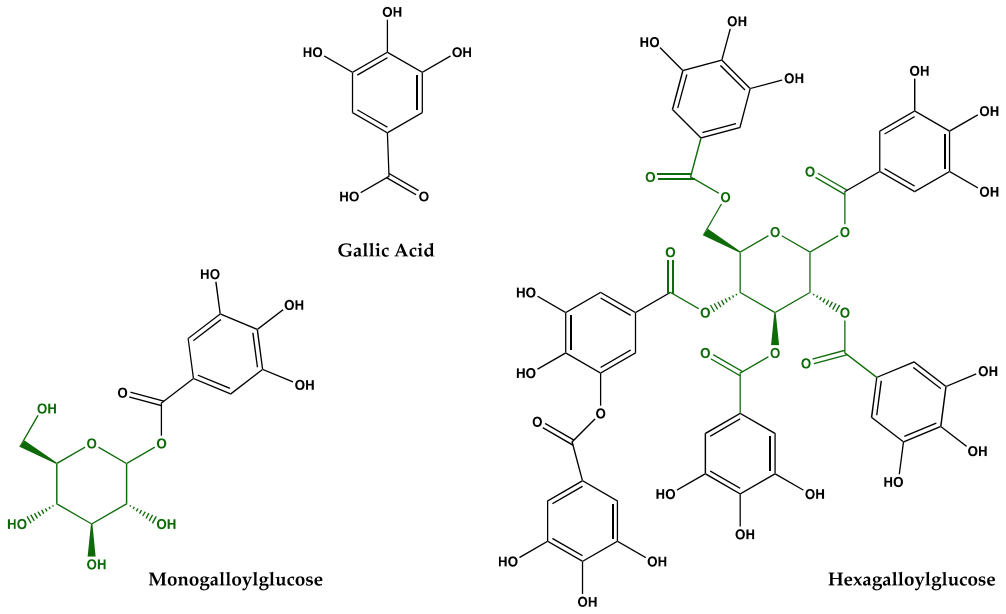

Figure 1. Chemical structures of gallic acid, monogalloyl glucose, and hexagalloyl glucose. For gallic acid, the main functional group is based on a carboxylic acid, and the others are based on an ester. Phenolic OH groups are also important in the formation of the iron(II)-phenol complex. The galloyl esters of glucose can also be referred to as gallotannins.

1.2. New Formulations Disclosed in the Past Through the Use of Historically Accurate Reconstructions for Iron Gall Inks

Since ancient times, historically accurate reconstructions of medieval inks have been crucial to bringing new insights into iron gall inks' complex structure and compounds formed within them [5,12,16]. Table 1 shows Iberian inks dated between the 15th and 17th centuries. These inks and two other black writing inks, QI.8 and QI.9, selected from the 13th-century Andalusian technical treatise, hold significant historical and chemical value.

Table 1. Extracts were prepared following the al-Qalalūsī and Iberian recipes. The concentration of gallic acid and the sum of pentagalloylglucose and hexagalloylglucose (PGG + HxGG), expressed in mg/mL of gallic acid equivalents, as well as their relative percentage.

Recipe	[Gallic Acid]	[PGG + HxGG]	Phenolic Compounds	% [Gallic Acid]/ Phenolic Compounds	% [PGG + HxGG]/ Phenolic Compounds
Braga	1.9 ± 0.6	15 ± 2	26 ± 3	7.7 ± 0.9	56 ± 2
Montpellier	5 ± 1	11 ± 1	27± 2	18 ± 2	40 ± 6
Córdoba	5 ± 1	0.15 ± 0.01	7 ± 4	65 ± 3	2.1 ± 0.8
Guadalupe	4 ± 1	32 ± 3	51± 4	8 ± 1	62 ± 3
Madrid	1.00 ± 0.04	11.5 ± 0.5	17.8 ± 0.6	5.6 ± 0.3	65 ± 1
QI.8	0.202 ± 0.002	1.94 ± 0.05	2.43 ± 0.07	8.3 ± 0.2	79.9 ± 0.2
QI.9	0.2085 ± 0.0009	2.250 ± 0.007	2.89 ± 0.02	7.22 ± 0.05	77.9 ± 0.5

They represent institutions where writing ink was essential, such as universities, notaries, chanceries, and the monastic world. Henceforth, the manuscripts and respective recipes will be designated as Braga, Montpellier, Córdoba, Guadalupe, Madrid, QI.8, and QI.9, respectively. QI.8 was obtained by infusion and QI.9 by decoction [16]. In this first aging study, we did not add gum arabic to these recipes to study their degradation products.

Table 1 depicts the main compounds in the extracts; for more information on these inks, please see references [5,12,16]. The results obtained by HPLC–DAD and HPLC–ESI–MS showed that PGG and HxGG were the compounds present in higher concentrations, except in the Córdoba recipe. Overall, the percentage of gallic acid in the phenolic extract was found to be higher for the extraction methods that used only water, as shown in Córdoba and Montpellier (Table 1). The other three recipes were prepared with different solvents or solvent mixtures: water and vinegar (Braga), water and wine (Guadalupe), or only wine (Madrid). It was very interesting to observe that wine was not the most efficient extraction method for phenolic compounds (17.8 ± 0.6 mg/mL) [12]. The best-performing extraction was achieved with a mixture of water and wine in a 1:0.25 proportion (51 ± 4 mg/mL); even a solution of water and vinegar (2:1) yielded better results than using only wine (26 ± 3 mg/mL) [12].

Considering the data in Table 1, we selected Montpellier and Guadalupe as the inks to be tested with the gels. We also included QI.8.

1.3. The Preservation of a Diversity of Iron Gall Inks

Developing safer and sustainable treatments, tailored as much as possible to the object, is crucial. Our microreview on conservation treatments highlights the significant advances made over the last decade in our understanding of the degradation mechanisms of iron gall inks [17–20]. This progress has significantly enhanced our ability to mitigate the degradation caused by iron gall inks, which induce cellulose scission through acid catalysis and/or redox reactions [21–29]. An overview of current conservation treatments to mitigate iron gall ink deterioration, from the late 19th century to the beginning of the 20th century, as well as current phytate and new postphytate treatments, can be found in references [30–39].

Piero Baglioni's group, a leader in the field of nanotechnology, has also studied stabilization treatments for iron gall inks. Their research led to the development of a combined deacidification and strengthening treatment. This treatment involves hydroalcoholic gelatine solutions (ethanol or isopropanol) mixed with $Ca(OH)_2$ nanoparticles called GeolNan, which has the potential to significantly increase the resistance of cellulose to hydrolysis and oxidation induced by iron gall ink [33–38]. However, due to the alkalinity of calcium hydroxide nanoparticles in the presence of moisture [34,39], it is of utmost importance to

exercise special caution and control the pH when treating heavily oxidized cellulose, such as iron gall ink corroded paper, to mitigate the higher risk of alkaline degradation.

1.4. Main Degradation Products of Iron Gall Inks

In a recent publication by Lerf et al., a significant breakthrough was made in studying historical documents using Mössbauer spectroscopy [40]. Three documents were examined: two damaged documents from a library in Granada (Chancery MS and Latin MS) and a book handwritten in German from the 18th century. The Chancery MS revealed the presence of Fe^{2+}-oxalate, possibly as $FeC_2O_4 \cdot 2H_2O$, and basic iron sulfates of the jarosite type, $(H_3O)Fe_3(SO4)_2(OH)_6$. The formation of oxalate, as Lerf et al. suggested, could be a result of binding media degradation [41,42] or cellulose degradation. This finding adds to the body of knowledge about Fe^{2+}-oxalates previously detected in ancient documents [43,44].

La Camera's work is also noteworthy in this field. By examining iron gall ink crystals in drawings dating from 15th to 19th-century Europe in the Department of Prints, Drawings, and Photographs of the Museum of Fine Arts Boston and selecting additional collections [45], La Camera proposed iron sulfates as degradation products. This finding adds to the growing body of knowledge on this subject.

Ferrer and Sistach contributed to the knowledge of the degradation products of iron gall inks based on their characterization of sediments found on the surface of writing inks in manuscripts dated between the 14th and 17th centuries [4]. The authors clearly showed that these sediments were probably degradation products of the writing inks. Calcium, copper, and Fe^{2+} oxalates were identified in samples with higher pH values and low degradation. On the other hand, magnesium and Fe^{3+} oxalates were detected in severely degraded inks. In addition to oxalates, an iron basic sulfate was identified in five samples, and a good match with amarantite ($FeSO_4OH \cdot 3H_2O$) was found; in two of these samples, minor ink corrosion was observed, but in the other three, strong ink corrosion was present [4,46,47].

1.5. How to Preserve Iron Gall Inks Using a Green Approach

New green policies have developed various methods to preserve iron gall inks. One of the first methods, developed by Ferrer et al., involves using phytic acid (inositol hexaphosphate), a molecule naturally produced by various plant species [4]. This natural compound allows for the chelation of excess Fe^{2+} ions and pH buffering, preventing the acidic degradation of paper.

The literature also reports different approaches based on alkaline nanostructures, such as the one developed by Baglioni et al. In recent decades, applied chemistry in cultural heritage has provided multiple approaches for restoring and preserving cultural assets. This research is paramount in our collective efforts to safeguard our cultural heritage [36].

Recent years have seen the introduction of several hydrogels for the preventive treatment of a wide range of cultural heritage materials, including frescoes, paintings, murals, stone surfaces, and metals. The use of hydrogels, a widely studied practice, underscores their versatility and potential in the field [48–51]. A hydrogel is a biphasic material composed of a solid phase, consisting of a natural or synthetic polymer, dispersed in a liquid phase. There are two types of gels: physical gels and chemical gels [52–54].

In physical gels, hydrogel formation is related to polymer–solvent interactions through weak forces such as Van der Waals forces, hydrogen bonds, dipole interactions, and ionic interactions (as in calcium alginate-based gels). On the other hand, strong chemical bonds, such as covalent bonds, promote the formation of chemical gels.

This study proposes an innovative approach: using a chemically crosslinked gel to remove unwanted materials from the ink surface. This novel method promises to significantly advance the preservation of iron gall inks and cultural heritage materials.

2. Materials and Methods

2.1. Preparation of the Extracts and Inks

The inks selected encompassed the highest variability between recipes: Braga, Montpellier, Guadalupe, Madrid, Qalalusi QI.8, and Qalalusi QI.9 [5,12,16]. Except for the galls, all reagents used were of analytical grade. Spectroscopic or equivalent grade solvents and Millipore water were used for all the chromatographic and spectroscopic studies. Gallnuts (oak apples from *Quercus infectoria*) were purchased from Kremer. White wine vinegar and organic white wine were acquired in a local organic supermarket.

A final volume of 50 mL of each ink was prepared without the addition of gum arabic. Of these 50 mL, 10 mL were placed in 100 mL Erlenmeyer flasks for the aging experiment, and the rest were kept in glass flasks at RT (21 °C) and protected from light.

The main steps and ingredients used to prepare the recipes. RT is room temperature.

	Water	Others	Galls	$FeSO_4$	Extraction	pH	
						Extr.	Final
Braga	99 mL	49.8 mL vinegar	9.36 g	37.5 g $FeSO_4$	Boiling and reduced to 1/3	2.84	1.73
Montpellier	200 mL		5.72 g	3.8 g $FeSO_4$	3 days at RT Boiling and reduced to ¼ Filtration	3.39	2.51
Guadalupe	37.5 mL	12.5 mL white wine	5.6 g	3.75 g $FeSO_4$ 1.87 g $CuSO_4$	6 days at RT Aquece 10 min Filtration	3.56	2.47
Madrid	-	50 mL white wine	2.76 g	2.76 g $FeSO_4$ 0.22 g Al^{3+}, indigo, sugar	6 days at RT Filtration	3.18	2.31
QI.8	50 mL	-	2.5 g	2.5 g $FeSO_4$	4 days at RT Filtration	3.86	2.29
QI.9	75 mL	-	6.15 g	4.95 g $FeSO_4$	24 h at RT Boiling and reduced to 2/3 Filtration	3.81	2.30

2.2. Aging

The Erlenmeyer flasks with the inks were placed in an orbital shaker (Optic-Ivymen model) at 150 rpm and 50 °C. For each analysis time, the Erlenmeyer was removed from the orbital shaker and placed under agitation to avoid precipitation of the complex due to the lack of gum arabic in a water bath at 50 °C. For analysis, 40 µL of ink was extracted using a micropipette and applied onto filter paper, in 2 cm^2 squares and glass slides. The inks were always applied as triplicates in both supports to ensure reproducibility.

2.3. HPLC–DAD and HPLC–ESI–MS

All samples were analyzed by HPLC–DAD, and the compounds were identified by HPLC–ESI–MS, as reported elsewhere [5]. HPLC–DAD analyses were performed in a Merck-Hitachi Elite LaChrom HPLC–DAD on a 150 × 4.6 mm i.d., 5 µm pore size

reversed-phase C18 col-umn (Merck) thermostated at 25 °C (Merck-Hitachi Column Oven L-2300). Detection was carried out at 280 nm using a diode array detector (Merck-Hitachi Diode Array Detector L-2455). The stationary phase was a LiChrospher RP-18 column (150 × 4.6 mm i.d., 5 µm) at 25 °C [55].

The mobile phases were composed of solvent A, 1% (*v*/*v*) formic acid, and solvent B, 100% (*v*/*v*) acetonitrile. The flow rate was 0.50 mL/min, the injection volume was 0.25 µL, and the gradient method started with a linear gradient ranging from 90% A to 65% A in 50 min, then reaching 100% B in 5 min, and a final isocratic gradient of 100% B during 7 min and a final re-equilibration isocratic gradient of 90% A for 5 min.

2.4. Colorimetry

L*, a*, and b* are the three color coordinates for the CIELab system. L* represents the Lightness, and a*, b* the Hue. L* variations range from "light", or white, to > 0, "dark", or black, < 0, on the *z*-axis; a* ranges from red to green; b* ranges from yellow to blue. a* > 0 represent reds, and a* < 0 represents greens. b* > 0 represents yellows, and b* > 0 represents blues.

The color measurements in 2025 were carried out using a handheld spectrophotometer Lovibond TR 520, with a diffused illumination system, an 8° viewing angle, and a 48 mm integrating sphere. The measuring aperture had a diameter of 4 mm. The equipment calibration was performed using white and black references. The color coordinates were calculated by defining the D65 illuminant and the 10° observer.

The measurements were performed by placing a cellulose-based paper under the inks to eliminate the influence of color from any underlying surfaces. It had the following coordinates L* = 98.33, a* = 0.09, and b* = 1.37. The measurements were repeated three times to ensure accuracy at a temperature of 20 ± 1 °C and a relative humidity of RH% = 60 ± 2. The equipment was from Tintometer, Dortmund, Germany.

2.5. Microscopy

The ink examination and micro-sampling were conducted under a Leica MZ16 stereomicroscope equipped with a Leica ICD digital camera and a fiber-optic light Leica system (Leica KI 1500 LCD), acquired in Lisbon, Portugal. A set of 10× ocular lenses and objectives ranging from 0.71× up to 11.5× magnification gave a total resolution between 7.1× and 115×.

The micro-samples were collected under the microscope using the following microtools from Ted Pella®: a micro chisel nº13603 attached to a micro graver oval nº13611. These tools were acquired at Redding, CA, USA (www.tedpella.com, accessed on 1 June 2025).

2.6. Micro-Infrared Spectroscopy

Infrared analyses were performed using a Nicolet Nexus spectrophotometer coupled to a Continuµm microscope (15 × objective) with an MCT-A detector. The spectra were collected in transmission mode, in 50 µm^2 areas, with a resolution setting of 4 or 8 cm^{-1} and 128 scans, using a Thermo diamond anvil compression cell. CO_2 absorption at ca 2400–2300 cm^{-1} was removed from the acquired spectra (4000–650 cm^{-1}). To improve the robustness of the results, at least two spectra were acquired from different sample spots.

2.7. Micro-Raman Spectroscopy

Raman microscopy was carried out using a Horiba Jobin–Yvon LabRAM 300 spectrometer, equipped with a diode laser with an excitation wavelength of 785 nm and a maximum laser power of 37 mW measured at the sample. Spectra were recorded as an extended scan. The laser beam was focused with a 50x Olympus objective lens, and the spot size was 4 µm. The laser power at the sample surface was between 9.5 and 0.37 mW. No evidence of

ink degradation was observed during spectra acquisition. More than three spectra were collected from the same sample. A silicon reference was used to calibrate the instrument.

2.8. Preparation of the Gels

A thin film and bulk material were developed through a casting process, SM4. The hydrogel preparation was optimized with qualitative tests. Silicone molds were used to control the shape during the freezing cycle. Hydrogel samples with two different shapes (film and "rough cube") were obtained. Polymer (0.5 g) was poured in a 20 mL vial with demineralized water (10 mL). The sealed vial was magnetically stirred at 60 °C for 20 h. After this period, the solution was poured into a silicone mold (about 2 × 2 cm^2) and placed in a freezer a −20 °C for 16 h. Then, the frozen polymer was removed from the mold and placed on Japanese paper until it was dry (approximately 24 h). To obtain the final hydrogel sample, the dried film was treated with the solution used for the cleaning.

3. Results and Discussion

3.1. Aging of the Iron Gall Inks

A multi-analytical approach was used to study the iron gall inks based on colorimetry, Raman infrared spectroscopies, and HPLC–DAD–MS. Using HPLC–DAD, inks and extracts for Braga, Montpellier Guadalupe, and Córdoba were quantified using the following irradiation times: 0 h, 20 h, 40 h, 78 h, 100 h, 172 h, 196 h, 220 h, 260 h, and 336 h. These extracts and inks were prepared without gum arabic. Based on colorimetry, Raman and infrared spectroscopies, Braga, Montpellier, Guadalupe, Madrid, QI.8, and QI.9 were studied for the following irradiation times: 0 h, 696 h, and 1959 h. Those inks were studied as precipitates applied on glass slides and filter paper. For more details, please see Materials and Methods (Section 2.2). Their t0 was acquired between July 2019 and early August 2019.

Montpellier, Guadalupe and QI.8 inks were selected for repair using gels. The first tests were performed on several Braga inks, prepared by former Ph.D. students in November 2018, and the data are available as Supplementary Material S4.

The aging experiments were carried out in an orbital shaker at 150 rpm and 50 °C. These were compared with inks at room temperature (21 °C) and protected from light.

3.2. Quantification of the Polyphenols Identified in the Inks by HPLC–DAD

The inks are discussed in this section; for the extracts, see Supplementary Material S1. In Table 2, we show the data for the Braga and Córdoba inks, expressed as gallic acid and the sum of pentagalloylglucose, hexagalloylglucose, and heptagalloylglucose (PGG + HxGG + HpGG), in mg/mL of equivalents of gallic acid, as well as their relative percentage. At the irradiation time of 336 h hours, we can observe that the PGG + HxGG + HpGG compounds were not detected, and that gallic acid in Braga was at 70% and Córdoba was at 87.6%. These data are discussed in the infrared and Raman sections, but an extended network has probably been created, making it challenging to detect PGG + HxGG + HpGG-based compounds. For Montpellier, a similar pattern is observed in Table 3. On the other hand, for Guadalupe, the percentage of gallic acid was 16.8%, and for the PGG + HxGG + HpGG, it was 56%, Table 3.

Table 2. Braga and Córdoba inks. The concentration of gallic acid and the sum of pentagalloylglucose, hexagalloylglucose, and heptagalloylglucose (PGG + HxGG + HpGG), expressed in mg/mL of equivalents of gallic acid, as well as their relative percentage.

Recipe	Irradiation Time	Gallic Acid	PGG + HxGG + HpGG	Phenolic Compounds	% [Gallic Acid]/Phenolic Compounds	% [PGG + HxGG + HpGG]/Phenolic Compounds
Braga	**0 h**	3.047 ± 0.006	9.5 ± 0.2	16.5 ± 0.3	18.4 ± 0.3	57 ± 2
	20 h	2.31 ± 0.02	2.3 ± 0.2	6.5 ± 0.3	36 ± 2	35 ± 3
	40 h	2.27 ± 0.01	0.93 ± 0.08	4.6 ± 0.1	50 ± 1	20 ± 2
	60 h	2.138 ± 0.008	1.95 ± 0.06	5.7 ± 0.1	37.8 ± 0.7	35 ± 1
	78 h	1.70 ± 0.02	1.09 ± 0.03	4.16 ± 0.07	40.9 ± 0.8	26 ± 1
	100 h	1.62 ± 0.04	0.5 ± 0.2	3.3 ± 0.4	49 ± 6	16 ± 6
	172 h	1.231 ± 0.004	0.12 ± 0.04	2.3 ± 0.2	53 ± 4	5 ± 2
	196 h	1.30 ± 0.01	0.08 ± 0.02	2.60 ± 0.07	50 ± 1	3.1 ± 0.6
	220 h	0.906 ± 0.004	0.140 ± 0.004	1.83 ± 0.03	49.5 ± 0.8	7.7 ± 0.2
	260 h	0.867 ± 0.002	0.007 ± 0.004	1.65 ± 0.03	53 ± 1	0.4 ± 0.3
	336 h	0.306 ± 0.006	nd *	0.44 ± 0.02	70 ± 3	nd *
Córdoba	**0 h**	5.00 ± 0.02	3.91 ± 0.06	11.3 ± 0.2	44.0 ± 0.7	34.4 ± 0.7
	20 h	3.16 ± 0.04	1.05 ± 0.01	5.0 ± 0.1	64 ± 2	21.0 ± 0.5
	40 h	3.37 ± 0.03	0.89 ± 0.01	5.24 ± 0.08	64 ± 1	17.0 ± 0.4
	60 h	3.74 ± 0.01	1.14 ± 0.02	6.12 ± 0.06	61.2 ± 0.6	18.7 ± 0.3
	78 h	2.47 ± 0.03	0.96 ± 0.04	4.5 ± 0.1	55 ± 2	21 ± 1
	100 h	2.63 ± 0.01	0.67 ± 0.01	4.54 ± 0.07	58.1 ± 0.9	14.8 ± 0.3
	172 h	1.77 ± 0.03	0.26 ± 0.05	2.9 ± 0.1	60 ± 3	9 ± 2
	196 h	1.77 ± 0.01	0.51 ± 0.02	3.36 ± 0.05	52.8 ± 0.9	15.2 ± 0.6
	220 h	1.83 ± 0.02	0.91 ± 0.03	4.3 ± 0.1	43 ± 1	21.4 ± 0.9
	260 h	3.21 ± 0.03	0.67 ± 0.01	5.22 ± 0.06	61.5 ± 0.9	12.9 ± 0.3

* nd—not detected.

Table 3. Guadalupe and Montpellier inks. The concentration of gallic acid and the sum of pentagalloylglucose, hexagalloylglucose, and heptagalloylglucose (PGG + HxGG + HpGG), expressed in mg/mL of equivalents of gallic acid, as well as their relative percentage.

Recipe	Irradiation Time	Gallic Acid	PGG + HxGG + HpGG	Phenolic Compounds	% [Gallic Acid]/Phenolic Compounds	% [PGG + HxGG + HpGG]/Phenolic Compounds
Guadalupe	**0 h**	1.975 ± 0.009	16.0 ± 0.2	21.7 ± 0.3	9.1 ± 0.1	74 ± 1
	20 h	1.42 ± 0.03	7.0 ± 0.2	9.7 ± 0.3	14.6 ± 0.6	72 ± 3
	40 h	1.467 ± 0.007	7.27 ± 0.06	10.5 ± 0.1	13.9 ± 0.2	69 ± 1
	60 h	1.31 ± 0.03	6.5 ± 0.1	9.3 ± 0.2	14.2 ± 0.4	70 ± 2
	78 h	1.21 ± 0.01	6.6 ± 0.1	9.5 ± 0.2	12.8 ± 0.3	70 ± 2
	100 h	1.575 ± 0.003	8.2 ± 0.2	12.0 ± 0.2	13.1 ± 0.2	68 ± 2
	172 h	1.771 ± 0.005	8.4 ± 0.1	12.8 ± 0.2	13.8 ± 0.2	66 ± 1
	196 h	1.58 ± 0.02	6.99 ± 0.09	10.9 ± 0.2	14.4 ± 0.3	64 ± 1
	220 h	1.29 ± 0.02	5.19 ± 0.09	8.6 ± 0.2	15.0 ± 0.4	61 ± 2
	260 h	1.147 ± 0.008	3.53 ± 0.03	6.17 ± 0.09	18.6 ± 0.3	57.2 ± 0.9
	336 h	0.581 ± 0.003	1.93 ± 0.04	3.46 ± 0.06	16.8 ± 0.3	56 ± 2

Table 3. *Cont.*

Recipe	Irradiation Time	Gallic Acid	PGG + HxGG + HpGG	Phenolic Compounds	% [Gallic Acid]/Phenolic Compounds	% [PGG + HxGG + HpGG]/Phenolic Compounds
Montpellier	**0 h**	7.06 ± 0.04	7.2 ± 0.2	27.7 ± 0.4	25.5 ± 0.4	26.0 ± 0.8
	20 h	6.02 ± 0.04	3.35 ± 0.06	15.1 ± 0.2	39.8 ± 0.7	22.2 ± 0.5
	40 h	5.71 ± 0.04	2.20 ± 0.02	12.0 ± 0.1	47.5 ± 0.5	18.3 ± 0.2
	60 h	5.76 ± 0.02	2.40 ± 0.04	13.1 ± 0.2	44.1 ± 0.6	18.4 ± 0.4
	78 h	5.27 ± 0.08	2.03 ± 0.07	11.2 ± 0.3	47 ± 1	18.1 ± 0.8
	100 h	5.67 ± 0.02	1.99 ± 0.05	11.7 ± 0.2	48.4 ± 0.7	17.0 ± 0.5
	172 h	6.1684 ± 0.0005	2.61 ± 0.02	15.26 ± 0.06	40.4 ± 0.2	17.1 ± 0.2
	196 h	3.342 ± 0.009	1.96 ± 0.06	10.0 ± 0.1	33.6 ± 0.5	19.7 ± 0.7
	220 h	5.38 ± 0.01	1.35 ± 0.02	11.4 ± 0.1	47.4 ± 0.6	11.9 ± 0.2
	260 h	4.47 ± 0.06	0.583 ± 0.007	8.0 ± 0.1	56 ± 1	7.3 ± 0.1
	336 h	4.650 ± 0.004	0.293 ± 0.005	7.47 ± 0.07	62.3 ± 0.6	3.92 ± 0.08

3.3. Infrared Spectra by Micro-Fourier Transform Infrared Spectroscopy

We started by depicting the infrared spectra for a series of precipitates based on iron complexes with gallate (iron gallate), digallate (iron–diGG), pentagallate (iron–PGG), and tannate (iron–tannate), Figure 2. The main markers were identified in orange, Table 4. For iron gallate, the marker bands were 1678 cm^{-1} and 1333 cm^{-1}. For iron–diGG, bands were at 1681 cm^{-1} and 1342 cm^{-1}. For iron–PGG, bands were at 1697 cm^{-1} and 1344 cm^{-1}. For iron–tannate, bands were at 1701 cm^{-1} and 1321 cm^{-1}. Based on these marker bands, we discuss the infrared spectra of the final recipes.

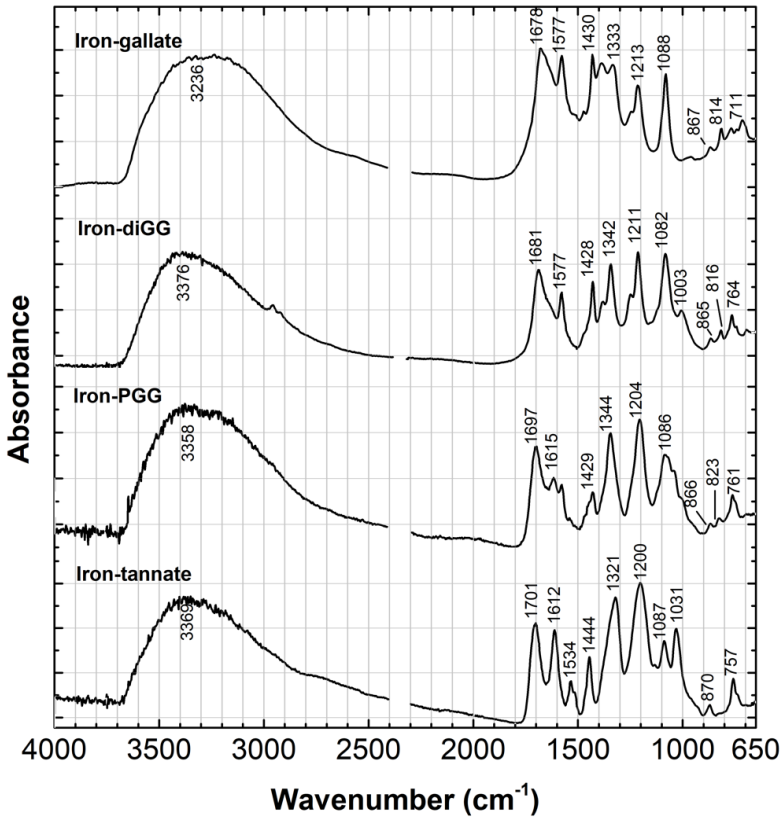

Figure 2. Infrared spectrum of iron gallate, di-gallate, penta-gallate, and tannate precipitates.

Table 4. Infrared bands for the selected inks, within orange the marker bands used to discuss their aging.

Braga	Montpellier	Guadalupe	Madrid	QI.8	QI.9	Assignments
759 *w*	761 *w*	759 *w*	757 *vw*	750 *vw*	760 *vw*	marker gallotannins
-	-	-	-	-	-	
871 *w*	870 *w*	871 *w*	871 *vw*	870 *vw*	870 *vw*	marker gallotannins
1035 *sh*	1042 *sh*	1035 *sh*	1040 *sh*	1040 *sh*	1040 *sh*	C-O str vib (ester)
1090 *s*	1094 *s*	1090 *s*	1093 *s*	1092 *s*	1091 *s*	marker gallotannins
1203 *m*	1204 *m*	1202 *m*	1203 *sh*	1204 *sh*	1204 *sh*	C-O str vib (ester)
1321 *m*	1325 *m*	1322 *m*	1323 *m*	1322 *m*	1321 *m*	C-O sym str (ester)
1446 *m*	1449 *m*	1448 *w*	1448 *w*	1448 *w*	1446 *w*	aromatic st vib
1540 *w*	1536 *w*	1536 *w*	1540 *sh*	1536 *sh*	1536 *sh*	n.a.
1615 *m*	1619 *m*	1613 *m*	1626 *m*	1615 *m*	1616 *m*	aromatic str vib
1704 *m*	1692 *m*	1708 *m*	1711 *sh*	1705 *sh*	1701 *sh*	C=O str (ester)
3352 *sh*	3361 *sh*	3363 *sh*	3353 *sh*	3367 *sh*	3359 *sh*	C-H str (polyphenols; gum arabic)

Table 4 describes the main bands, and Figure 3 shows the infrared spectra for t = 0 h, t = 693 h, and t = 1959 h.

The Braga ink, at t0, showed marker bands at 1704 cm^{-1} and 1321 cm^{-1}, which were close to the iron–tannate complex. At t = 693 h, we can see considerable degradation, and at t = 1959 h, the main compound was iron sulfate.

The Montpellier ink, at t0, showed marker bands at 1692 cm^{-1} and 1325 cm^{-1}, suggesting a mixture of several precipitates or a complex network, possibly iron–PGG and iron–tannate, together with iron sulfate. At t = 693 h, we can see a shift towards 1700 cm^{-1} and 1334 cm^{-1}, and at t = 1959 h, the bands were similar at 1697 cm^{-1} and 1333 cm^{-1}, together with a lower amount of iron sulfate. Compared to the Braga ink, this compound was more resilient.

The Guadalupe ink, at t0, showed marker bands at 1708 cm^{-1} and 1322 cm^{-1}, suggesting a mixture of several precipitates or a complex network, possibly iron–PGG and iron–tannate, together with iron sulfate. At t = 693 h, we can see a shift towards 1700 cm^{-1} and 1326 cm^{-1}; at t = 1959 h, the bands shifted again towards 1693 cm^{-1} and 1324 cm^{-1}, together with iron sulfate. Again, compared to the Braga ink, this compound has been better preserved.

The Madrid ink, at t0, showed marker bands at 1711 cm^{-1} and 1323 cm^{-1}, suggesting a mixture of several precipitates or a complex network, possibly iron–PGG and iron–tannate, together with iron sulfate. At t = 693 h, we can see a shift towards 1702 cm^{-1} and 1328 cm^{-1}; at t = 1959 h, the bands shifted again towards 1692 cm^{-1} and 1329 cm^{-1}, together with iron sulfate. Again, compared to the Braga ink, this compound suffered less degradation.

The Q.I8 ink, at t0, showed marker bands at 1705 cm^{-1} and 1322 cm^{-1}, closer to an iron-tannate complex or a complex network, together with iron sulfate. At t = 693 h, we can see a shift towards 1701 cm^{-1} and 1332 cm^{-1}; at t = 1959 h, the bands shifted again towards 1699 cm^{-1} and 1336 cm^{-1}, together with iron sulfate. Again, compared to the Braga ink, this compound was one of the most stable.

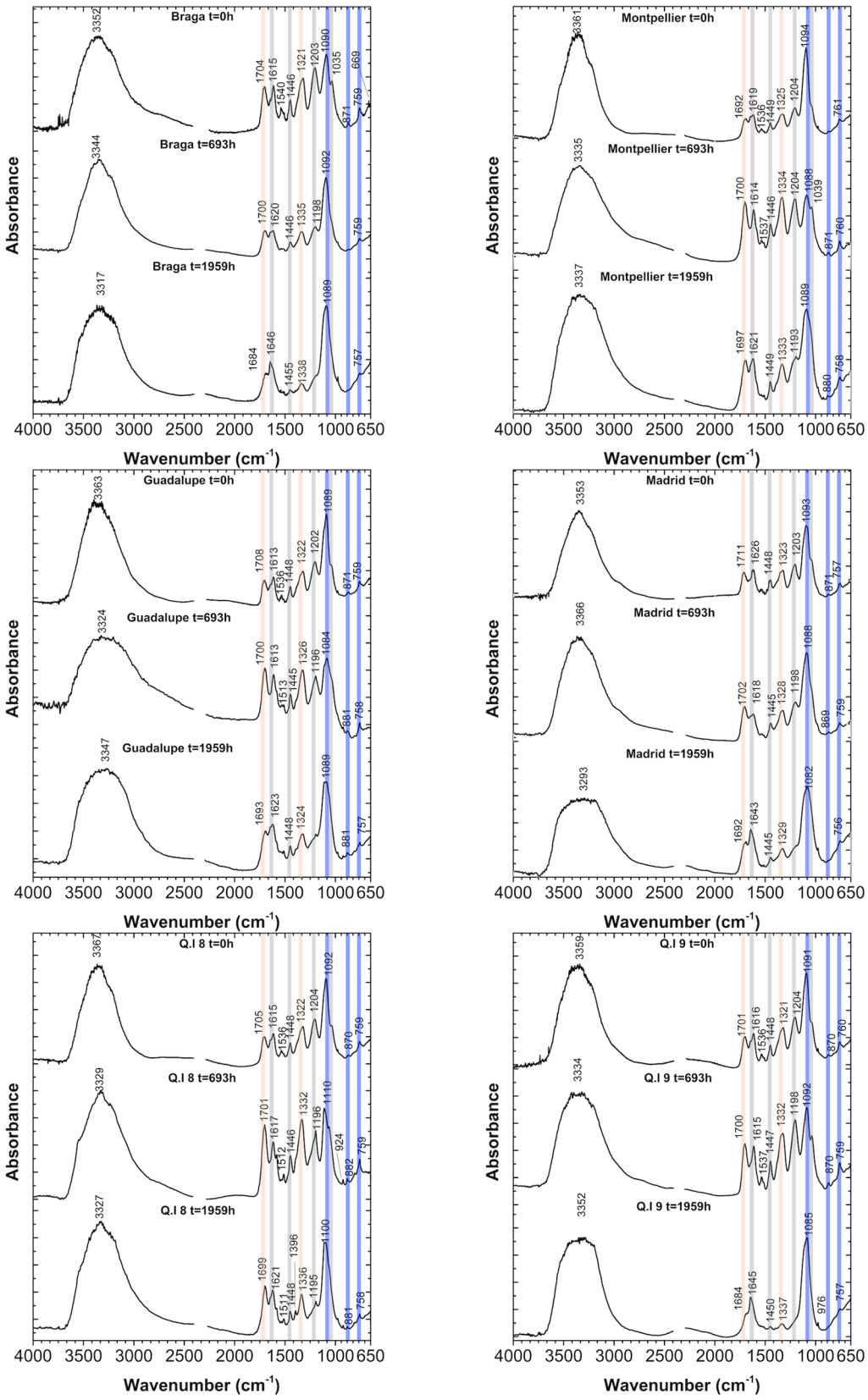

Figure 3. Infrared spectra for the following inks: Braga, Montpellier, Guadalupe, Madrid, QI.8, and QI.9, at t = 0 h, t = 693 h, and t = 1959 h. Studied as precipitates on a glass slide. For the meaning of the color bars, see Table 4.

The Q.I9 ink, at t0, showed marker bands at 1701 cm^{-1} and 1321 cm^{-1}, closer to an iron–tannate complex or a complex network, together with iron sulfate. At t = 693 h, we

can see a small shift towards 1700 cm^{-1} and a bigger shift towards 1332 cm^{-1}; at t = 1959 h, the bands shift again towards 1684 cm^{-1} and 1337 cm^{-1}, together with iron sulfate. Again, this compound showed a similar profile compared to the Braga ink.

Overall, the infrared spectra for t0 of Montpellier, Guadalupe, and QI8 were similar, varying in the amount of iron sulfate. These inks also aged better than the Braga and QI.9 inks. The precipitates formed can be big clusters.

When comparing these ink applications with the results obtained by HPLC–DAD, we may assume that only the products that are not polymerized can be identified.

3.4. Raman Spectra by Micro-Raman Spectroscopy

Contrary to what was observed in the infrared spectra, here, the Braga ink was the most resilient.

In Figure 4, we can verify the different behaviors of the paints in the degradation experiment using Raman spectroscopy. At t = 693 h, the inks were in good condition. However, at t = 1959 h, the most degraded inks were Montpellier, Guadalupe, Madrid, and QI.9. During the last degradation period, a spectrum of the Guadalupe ink could not be obtained. The only blacks that maintained the profile and bands corresponding to an iron gall ink were the Braga and QI.8 [5,16].

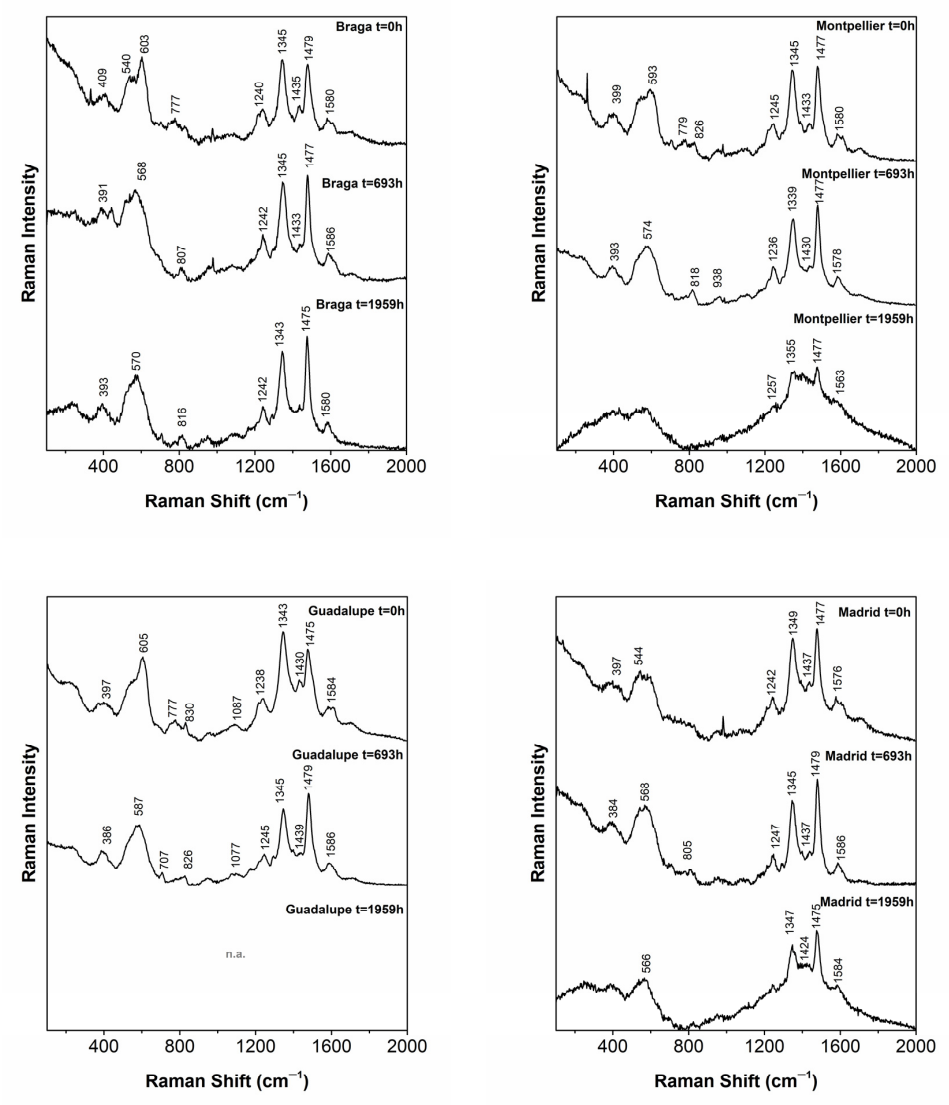

Figure 4. *Cont.*

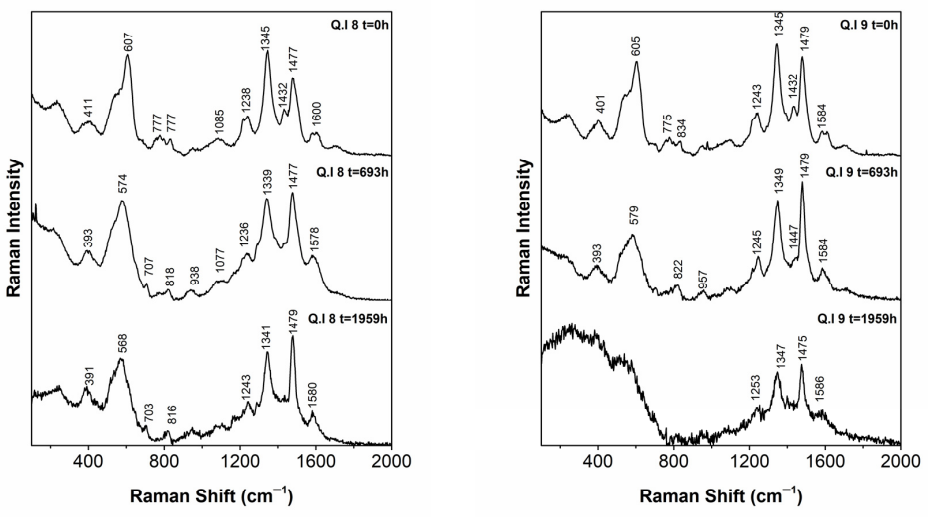

Figure 4. Raman spectra for the following inks: Braga, Montpellier, Guadalupe, Madrid, QI.8, and QI.9, at t = 0 h, t = 693 h, and t = 1959 h. Studied as precipitates on a glass slide.

3.5. Colorimetry Through L a* b* Coordinates*

The data for the experiments carried out in 2019 can be assessed in Supplementary Material S3 (Section 3.1). We show the present color coordinates for the aging experiments in an orbital shaker at 150 rpm and 50 °C in 2025 in Table 5. These were compared with inks at room temperature (21 °C) and protected from light, as shown in Table 6. All the L*a*b* coordinates acquired are shown in Supplementary Material S3 (Section 3.2).

Table 5. The colorimetric coordinates L*, a*, and b* of the inks for the aging experiments in an orbital shaker at 150 rpm and 50 °C. The inks were applied on filter paper.

	0 h			693 h			1959 h		
Refs	**L***	**a***	**b***	**L***	**a***	**b***	**L***	**a***	**b***
Braga	30.8 ± 0.7	−0.40 ± 0.05	−1.4 ± 0.1	22 ± 2	−0.2 ± 0.3	−1.0 ± 0.5	23 ± 3	−0.02 ± 0.2	0.2 ± 0.4
Montpellier	28.4 ± 0.8	0.27 ± 0.02	−1.4 ± 0.2	30.0 ± 0.6	0.7 ± 0.1	0.7 ± 0.2	32 ± 2	0.5 ± 0.2	1.9 ± 0.4
Guadalupe	28 ± 2	−0.5 ± 0.3	−1.8 ± 0.3	23 ± 2	0.36 ± 0.07	−0.3 ± 0.2	27 ± 2	0.2 ± 0.3	1.9 ± 0.6
Madrid	24 ± 1	0.4 ± 0.2	−0.2 ± 0.2	22 ± 1	0.6 ± 0.2	−0.3 ± 0.1	29 ± 5	0.2 ± 0.1	1.0 ± 0.5
QI.8	24 ± 2	0.1 ± 0.2	−3.04 ± 0.04	23 ± 4	0.11 ± 0.08	−1.0 ± 0.6	23 ± 6	−0.1 ± 0.2	2 ± 2
QI.9	25 ± 2	0.1 ± 0.3	−2.9 ± 0.7	22 ± 1	0.6 ± 0.2	−0.3 ± 0.1	23 ± 2	0.36 ± 0.07	−0.3 ± 0.2

Table 6. The colorimetric coordinates L*, a*, and b* of the inks at room temperature (21 °C) and protected from light. The inks were applied on filter paper.

	0 h			693 h			1959 h		
Refs	**L***	**a***	**b***	**L***	**a***	**b***	**L***	**a***	**b***
Braga	30.8 ± 0.7	−0.40 ± 0.05	−1.4 ± 0.1	18.4 ± 0.5	0.8 ± 0.2	−4.4 ± 0.6	19 ± 3	0.5 ± 0.4	−3.5 ± 0.7
Montpellier	28.4 ± 0.8	0.27 ± 0.02	−1.4 ± 0.2	23.7 ± 0.4	0.8 ± 0.07	−0.3 ± 0.3	22.7 ± 0.8	0.8 ± 0.1	−0.1 ± 0.2
Guadalupe	28 ± 2	−0.5 ± 0.3	−1.8 ± 0.3	19 ± 2	0.8 ± 0.3	−1.0 ± 0.2	19 ± 2	0.3 ± 0.1	−1.3 ± 0.1
Madrid	24 ± 1	0.4 ± 0.2	−0.2 ± 0.2	23 ± 1	0.7 ± 0.1	−2.4 ± 0.3	17.4 ± 0.6	0.84 ± 0.05	−2.7 ± 0.1
QI.8	24 ± 2	0.1 ± 0.2	−3.04 ± 0.04	29 ± 2	0.20 ± 0.03	−1.0 ± 0.7	31 ± 8	−0.4 ± 0.5	−0.2 ± 1.1
QI.9	25 ± 2	0.1 ± 0.3	−2.9 ± 0.7	23 ± 2	0.3 ± 0.2	−1.43 ± 0.08	18 ± 2	0.4 ± 0.4	−1.7 ± 0.2

Colorimetry was performed to determine the variation in color for Braga, Montpellier, Guadalupe, Madrid, QI.8, and QI.9. The L*a*b* coordinates allowed us to correlate the aging of the iron gall inks, as shown in Table 5. Concerning the L* coordinates and the aging time of 1959 h, Braga was the only ink that darkened; Montpellier and Madrid increased the lightness, and Guadalupe, QI.8, and QI.9 did not present significant changes. The a* values did not show a considerable variation. In contrary, the b* values changed from blue to yellow.

In Table 6, the data acquired at room temperature (21 °C) and protected from light show that the b* coordinate was still in the blue; the a* coordinate did not show relevant changes. Contrarily, the L* coordinate changed considerably. Braga's ink was blacker (from 30.8 to 19). For Montpellier, Guadalupe, Madrid, and QI.9, the values also decreased, but with a lower impact. The L* coordinate in QI.8 increased from 24 to 31.

3.6. Novel Green Approaches

The gels were tested and experimented on January and February 2025 as shown in Figure 5. Infrared spectra were acquired on the samples used for the gels, and the data are presented below.

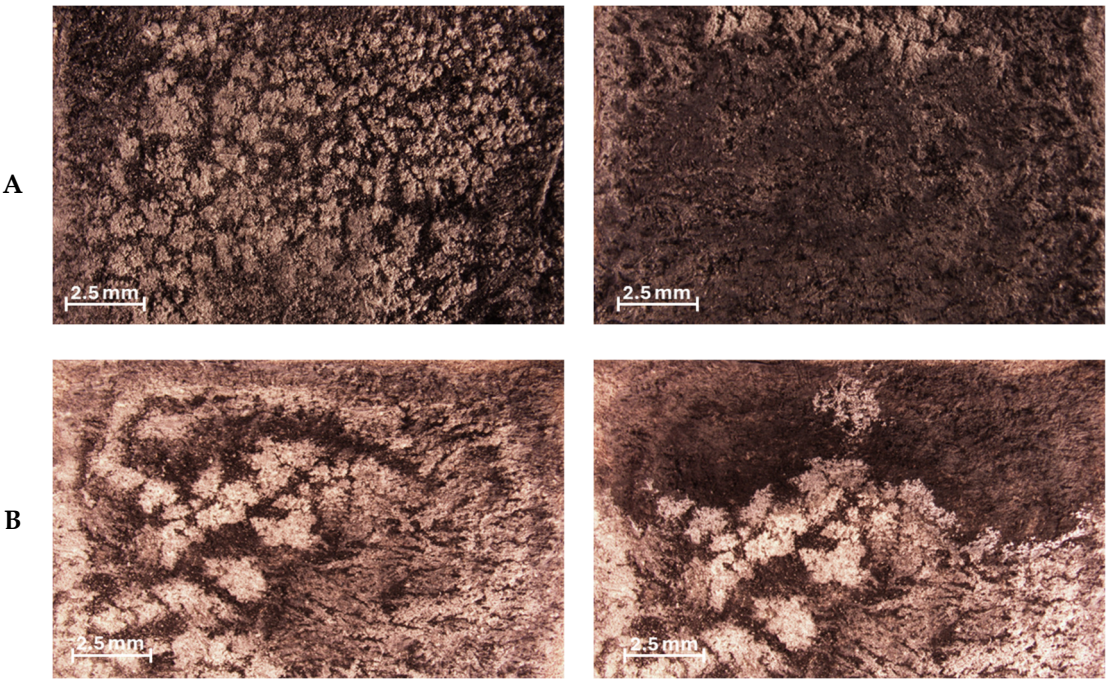

Figure 5. The gel was tested on Braga ink for 30 s for mockup (**A**) and 1 min for mockup (**B**) (before left, after right). The main degradation product, iron sulfate, was removed, indicating the cleaning effect of the gel. For more details, please see the text.

3.6.1. First Experimentation

The first tests were performed on an ancient Braga ink prepared in November 2018, in which the main degradation product was iron sulfate, identified by microFTIR (Supplementary Material S2, Figure S1). The selected solvent was a 10% ethanol in water that was included in the gel. To remove the iron sulfate with the gel, 15 s were sufficient.

Montpellier, Guadalupe, and QI.8 inks, aged during 1959 h, were analyzed in February 2025, Figure 6. These inks were applied on filter paper. The main degradation product found in these three inks was a match for an iron complex with ellagic acid, as shown in Figure 6.

For Montpellier ink, it was possible to acquire infrared spectra at time 0 and 1959 h, with the latter for the ink in the dark at room temperature and for the ink aged in the orbital shaker at 50 °C, as shown in Figure 7. When comparing the t0 of the present ink with the first spectra acquired on a glass slide, it is possible to see that the general features were there, with other products present, such as di- or/a pentagalloyl glucose complexes with iron, as shown in Figure 7, possibly within a complex network.

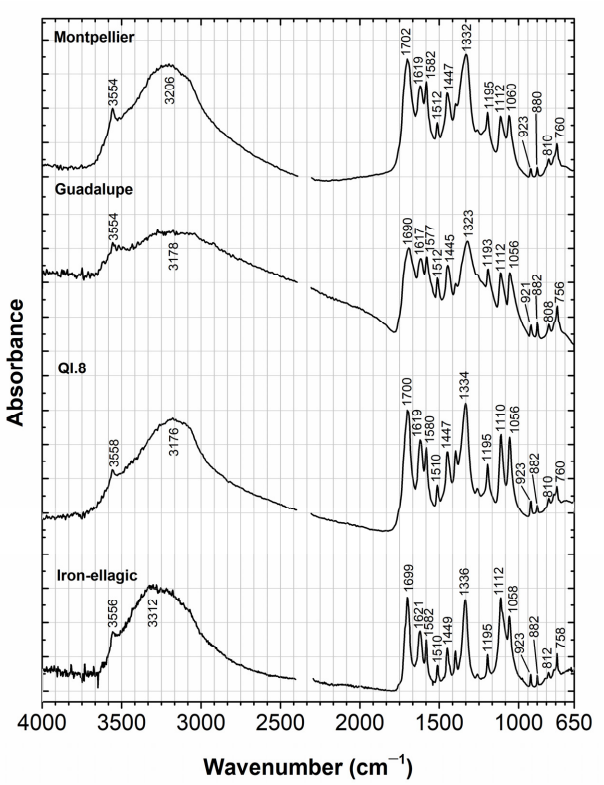

Figure 6. Infrared spectra for degradation products at 1959 h (orbital shaker at 50 °C), for Montpellier, Guadalupe, and QI.8 applied on filter paper. Compared with a complex of iron with ellagic acid.

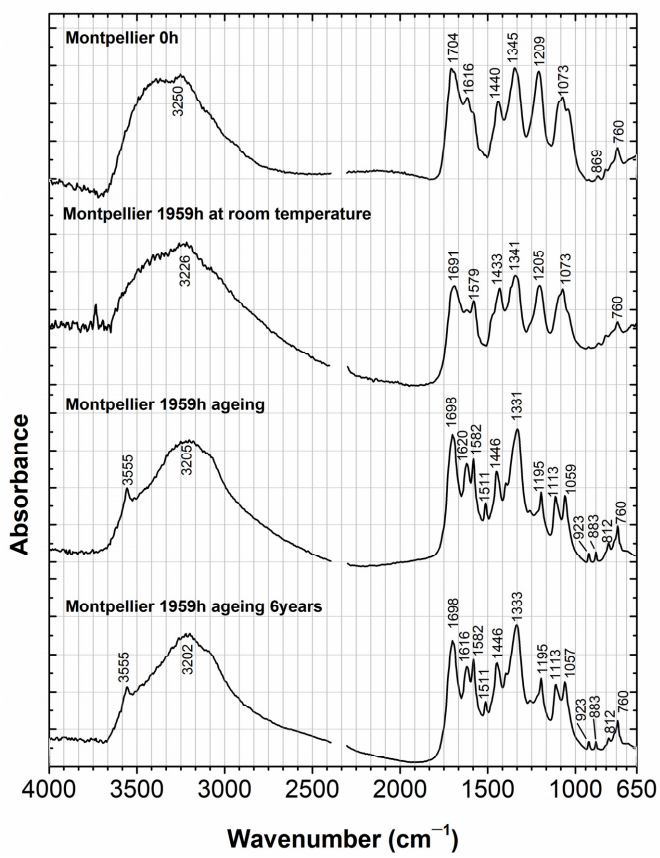

Figure 7. Infrared spectra for Montpellier applied to filter paper. Montpellier at t0 and t1959 h dark (protected at room temperature) and two spectra with aging at 50 °C, acquired after 6 years.

3.6.2. Cleaning Inks Through a Safe Approach

Experimentation with the gels was performed for 15 s, 30 s, 1 min, and 2 min, as shown in Figures 8 and 9. Guadalupe was the ink for which 1 min were enough. For the Montpellier and QI.8 inks, times in the order of 2 × 1 min were necessary. With these gels, it was possible to remove carefully the degradation products and to keep the inks safe, as shown in Figure 9.

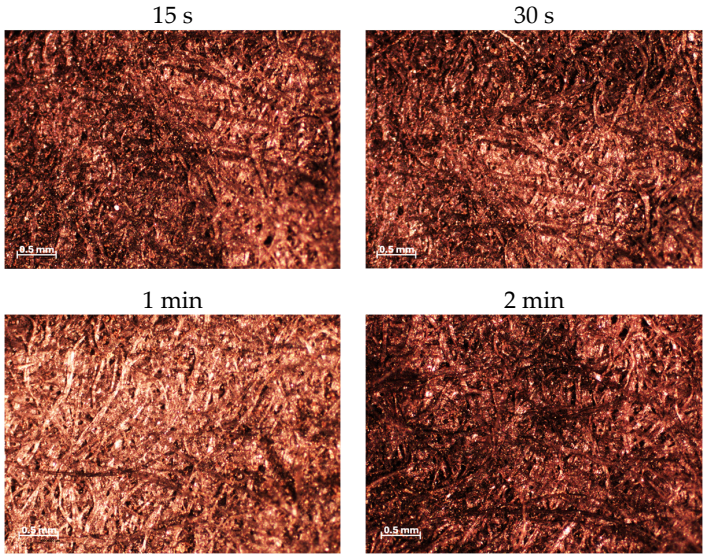

Figure 8. Montpellier ink at different time applications.

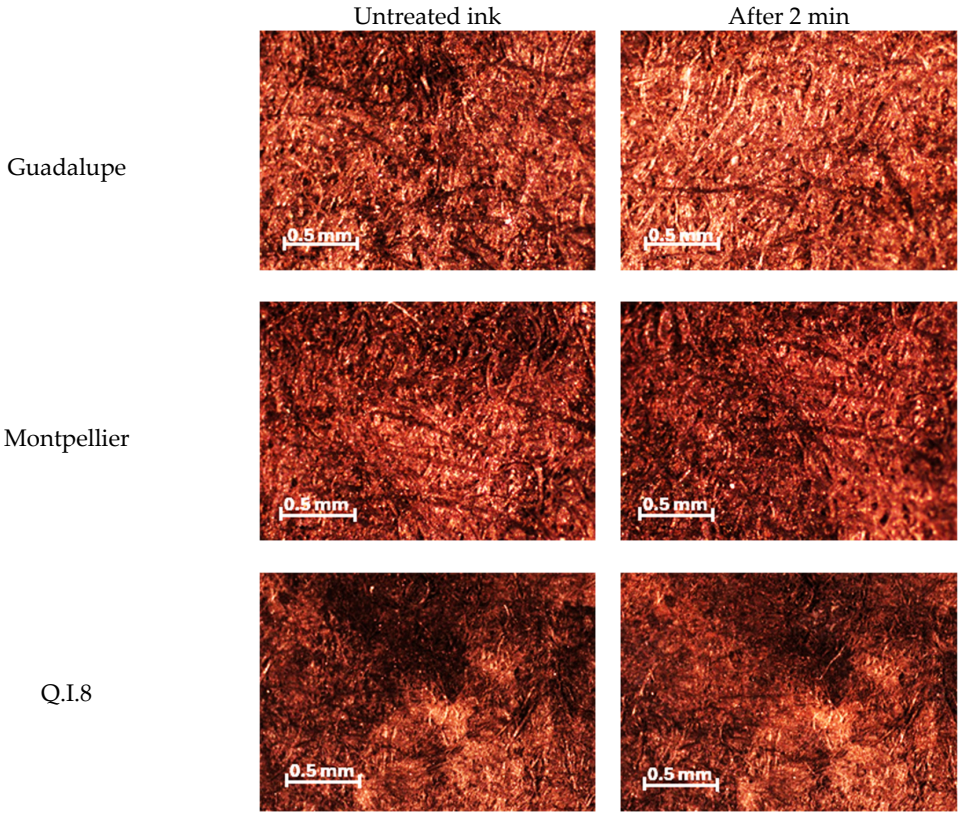

Figure 9. Images and times before and after Guadalupe, Montpellier, and QI.8 inks. Inks before and after two minutes of application.

After experimenting with small 2.5 × 3.5 mm pieces of gels, a larger gel was applied to Montpellier and QI.8 inks. These larger gels can be more efficient, but applying the smaller pieces may allow better control of the overall process. The larger gel can be described as "spongeous", being easy to apply, as shown as Figure 9.

For Montpellier, we also tested the same gel with a 10% aqueous solution of ethanol and 1% acetic acid, as shown in Figure 10. This gel was more rigid, and it was necessary to use a grinding pestle glass to improve the contact, the gel was applied two times. The gel containing the acidic solution was applied twice. In Figure 10a, the untreated ink is shown; in Figure 10b, the ink is shown after a 2 min treatment; and in Figure 10c, the ink is shown after the second 2 min treatment.

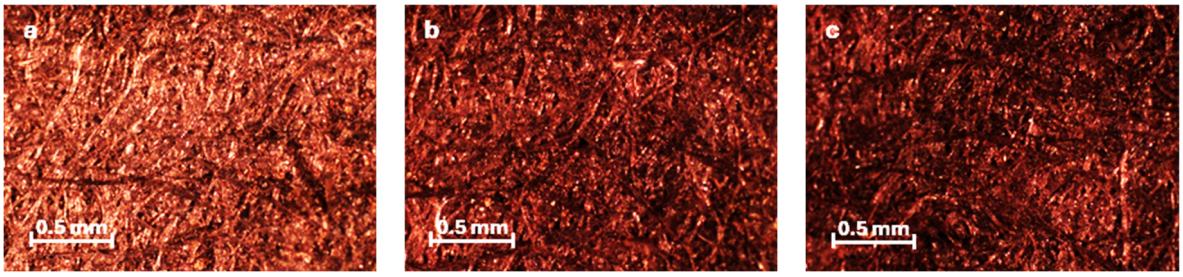

Figure 10. Images and times before and after Montpellier, with acid gel. (**a**) The untreated ink; (**b**,**c**) the ink after the second treatment.

Table 7 presents the colorimetry values for the following samples: Montpellier (Figure 8), treated with a 9:1 water–ethanol solution, and Montpellier (Figure 10) and Q.I.8, treated with a 9:1 water–ethanol solution with the addition of 1% acetic acid.

Table 7. The colorimetric coordinates L*, a*, and b* of the inks for the aging experiments in an orbital shaker at 150 rpm and 50 °C. The inks, applied on filter paper, were measured in February 2025.

	Before			After		
	L*	**a***	**b***	**L***	**a***	**b***
Montpellier Figure 9	32 ±1	0.65 ± 0.06	2.25 ± 0.05	31.3 ± 0.4	1.24 ± 0.05	2.73 ± 0.04
Montpellier Figure 10	31.63 ±0.01	0.18 ± 0.04	1.86 ± 0.07	30.3 ± 0.3	1.45 ± 0.07	2.26 ± 0.05
QI.8	24.3 ± 0.2	−0.01 ± 0.02	−1.04 ± 0.07	26.0 ±0.2	0.19 ± 0.01	0.9 ± 0.1

For the Montpellier color, a reduction in the L* parameter was observed in both cases, indicating that the ink regained a darker shade after treatment. Conversely, the Q.I.8 color showed an increase in colorimetric values, suggesting a shift towards lighter tones. The red values for the a* coordinate increased slightly. The b* coordinates also increased slightly towards yellow.

4. Conclusions

In this pioneering work, we aged five Iberian inks from the 15th to 17th centuries, along with two Arabic black writing inks, QI.8 and QI.9, from the 12th century. These inks, prepared in July and August 2019, were subjected to a multi-analytical approach using HPLC–DAD–MS, microFTIR, and microRaman techniques. The aged inks were carefully applied to filter paper for specific aging times: 0 h, 693 h, and 1959 h. The infrared spectra of the precipitates for t0 of Montpellier, Guadalupe, and QI8 were similar, varying in the amount of iron sulfate. Through their infrared spectra, these inks aged better than the Braga and QI.9 inks. The inks may evolve into significant clusters. When comparing these ink applications with the results obtained by HPLC–DAD, we may assume that only the

products that were not polymerized could be identified. This was confirmed by the work by Lerf and Wagner, who proposed that iron oxyhydroxides best represent the iron clusters and that these nanoparticles are "covered by a shell of polymerized oxidation products of the phenols".

In February 2025, we acquired infrared spectra of the inks applied to filter paper to understand the products formed during these six years. Our findings revealed two main degradation products: iron sulfate in the Braga ink and a complex of iron with ellagic acid for Montpellier, Guadalupe, and QI.8 inks. This study proposes an innovative approach: using a chemically crosslinked gel to remove unwanted materials from the ink surface. We conducted several tests to clean these degradation products using these gels, and our results have practical implications for the conservation of historical documents and artworks. For instance, the Braga ink was effectively cleaned with 10% ethanol in water, which was included in the gel, removing the iron sulfate within 15 s of application. On the other hand, the complex of iron with ellagic acid required longer application times, with successful removal after 2 min of application.

The advantages of each analytical technique, particularly microFTIR and microRaman, showed different results. The infrared spectra for Montpellier, Guadalupe, and QI8 aged better than the Braga and QI.9 inks. However, contrary to what was observed in the infrared spectra, the Braga ink was the most resilient in the Raman spectra.

Supplementary Materials: The following supporting information can be downloaded at: https://www.mdpi.com/article/10.3390/heritage8070261/s1, Figure S1: Infrared spectra of Braga ink prepared in November 2018, compared with the main degradation product, an iron sulfate. Two points were selected in different places of the ink (a,b), showing the iron sulfate. The black ink was acquired at a point in which iron sulfate was not so relevant (c); Figure S2: Under a microscope, micro-tools were used to acquire invisible micro-samples at points a and b, in which iron sulfate dominates. Another point was carefully selected to avoid the presence of iron sulfate for comparison; Figure S3: Infrared spectra of Montpellier, Guadalupe and QI.8 inks, acquired at t0 on July 2019; Figure S4: Comparison of the colorimetric coordinates a* and b* of iron-gall inks at t = 0 h; Figure S5a: Comparison of the colorimetric coordinates L* and a* of iron-gall inks; Figure S5b: Comparison of the colorimetric coordinates L* and b* of iron-gall inks; Figure S6: Object used to apply pressure on the polymer; Figure S7: Gel before and after the first, second, and third application on the ink surface; Figure S8: Gel applied to different inks after one application with the water-ethanol 9:1 mixture; Table S1: Extracts prepared following the Iberian recipes. Concentration of gallic acid and sum of pentagalloylglucose, hexagalloylglucose, and heptagalloylglucose (PGG + HxGG + HpGG), ex-pressed in mg/mL of equivalents of gallic acid, as well as their relative percentage; Table S2: Colorimetry of paints applied to filter paper; Table S3: The colorimetric coordinates L*, a*, and b* of inks were measured three times during aging experiments in an orbital shaker at 150 rpm and 50 °C. The measurements were repeated three times on three different days. For t = 0, the measurements were taken in the central part of the mock-ups (center), in the upper left part (up), and in the lower right part (down). The replica numbers indicate the days on which the measurements were performed. The measurements at t = 693 and t = 1959 were carried out on three different depositions (A, B, C) and repeated three times on other days; Table S4: The colorimetric coordinates L*, a*, and b* of the inks were measured three times during aging experiments conducted in an orbital shaker at 150 rpm at room temperature (21 °C), with the samples protected from light using an aluminum cover. The measurements were repeated three times on three different days. For t = 0, the measurements were taken in the central part of the mock-ups (center), in the upper left part (up), and in the lower right part (down). The replica numbers indicate the days on which the measurements were performed. The measurements at t = 693 and t = 1959 were carried out on three different depositions (A, B, C) and repeated three times on other days; Table S5: Mean and Standard Deviation of the Colorimetric Coordinates L*, a*, and b* of the iron-gall inks. The aging process was conducted in an orbital shaker at 150 rpm and 50 °C. The table presents the measurements at t = 693, taken on the first analysis day

(1st, 2nd, 3rd); Table S6: Mean and Standard Deviation of the Colorimetric Coordinates L*, a*, and b* of the iron-gall inks. The aging process was conducted in an orbital shaker at 150 rpm at room temperature (21 °C), with the samples protected from light using an aluminum cover. The table presents the measurements at t = 693, taken on the first analysis day on three different mock-ups (1st, 2nd, 3rd); Table S7: Mean and Standard Deviation of the Colorimetric Coordinates L*, a*, and b* of the iron-gall inks. The aging process was conducted in an orbital shaker at 150 rpm and 50 °C. The table presents the measurements at t = 1959, taken on the first analysis day (1st, 2nd, 3rd); Table S8: Mean and Standard Deviation of the Colorimetric Coordinates L*, a*, and b* of the iron-gall inks. The aging process was conducted in an orbital shaker at 150 rpm at room temperature (21 °C), with the samples protected from light using an aluminum cover. The table presents the measurements at t = 1959, taken on the first analysis day (1st, 2nd, 3rd); Table S9: Internal and surface pH values with the two different loading solutions; Table S10: L*, a*, b* parameters with corresponding mean and standard deviation before and after gel application.

Author Contributions: R.J.D.H. prepared the ink recipes. N.T. analyzed the extracts and inks by HPLC–DAD and HPLC–ESI–MS. P.N., V.O. and M.J.M. acquired and interpreted the infrared and Raman data. M.F. and M.L. prepared the gel to clean the degraded inks. M.J.M. prepared the original draft based on the reports by N.T., P.N., V.O. and M.J.M. Writing, review, and editing were performed by all authors. All authors have read and agreed to the published version of the manuscript.

Funding: This work received support and help from FCT/MCTES through national funds; LA/P/0008/2023 DOI 10.54499/LA/P/0008/2020, UIDP/50006/2020 DOI 10.54499/UIDP/50006/2023 and UIDB/50006/2023 DOI 10.54499/UIDB/50006/2023; PTDC/QUI-OUT/29925/2017; 2023.06024.CEECIND/CP2842/CT0010; 2021.01344.CEECIND/CP1657/CT0028 and CEECIND/01344/2021. The support from the Italian "Ministero dell'Università e della Ricerca" (MUR) and the University of Pavia through the program "Dipartimenti di Eccellenza 2023–2027" is acknowledged. This research was funded by the European Union—NextGenerationEU (Missione 4 Componente 1 CUP F13C22000840007).

Data Availability Statement: Most of the data on which the manuscript's conclusions rely are published in this paper, and the complete data are available for consultation on request to Maria J. Melo.

Acknowledgments: Mila Crippa's kindness and support are gratefully acknowledged for the colorimetry studies.

Conflicts of Interest: The authors declare no conflicts of interest.

References

1. Kolar, J.; Strlic, M. *Iron Gall Inks: On Manufacture, Characterisation, Degradation and Stabilisation*, 1st ed.; National and University Library of Slovenia: Ljubljana, Republic of Slovenia, 2006.
2. Bat-Yehouda, M.Z. *Les Encres Noires au Moyen Âge (Jusqu'à 1600)*, 1st ed.; CNRS Éditions: Paris, France, 1983.
3. Rouchon, V.; Bernard, S. Mapping iron gall ink penetration within paper fibres using scanning transmission X-ray microscopy. *J. Anal. At. Spectrom.* **2015**, *30*, 635–641. [CrossRef]
4. Ferrer, N.; Carme Sistach, M. Analysis of sediments on iron gall inks in manuscripts. *Restaurator* **2013**, *34*, 175–193.
5. Díaz Hidalgo, R.J.; Córdoba, R.; Nabais, P.; Silva, V.; Melo, M.J.; Pina, F.; Teixeira, N.; Freitas, V. New insights into iron-gall inks through the use of historically accurate reconstructions. *Herit. Sci.* **2018**, *6*, 1–15. [CrossRef]
6. Quideau, S.; Deffieux, D.; Douat-Casassus, C.; Pouységu, L. Plant Polyphenols: Chemical Properties, Biological Activities, and Synthesis. *Angew. Chem. Int. Ed.* **2011**, *50*, 586–621. [CrossRef]
7. Sylla, T.; Pouységu, L.; Da Costa, G.; Deffieux, D.; Monti, J.P.; Quideau, S. Gallotannins and Tannic Acid: First Chemical Syntheses and In Vitro Inhibitory Activity on Alzheimer's Amyloid b-Peptide Aggregation. *Angew. Chem. Int. Ed.* **2015**, *54*, 8217–8221. [CrossRef]
8. Stijnman, A. Iron gall ink in history: Ingredients and production. In *Iron Gall Inks Manuf Characterisation, Degrad Stabilisation*; Kolar, J., Strlic, M., Eds.; National and University Library of Slovenia: Ljubljana, Slovenia, 2006; Volume 1, pp. 25–67.
9. Liu, Y.; Fearn, T.; Strlič, M. Photodegradation of iron gall ink affected by oxygen, humidity and visible radiation. *Dye Pigment.* **2022**, *198*, 109947. [CrossRef]

10. Ponce, A.; Brostoff, L.B.; Gibbons, S.K.; Zavalij, P.; Viragh, C.; Hooper, J.; Alnemrat, S.; Gaskell, K.J.; Eichhorn, B. Elucidation of the Fe(III) Gallate Structure in Historical Iron Gall Ink. *Anal. Chem.* **2016**, *88*, 5152–5158. [CrossRef]
11. Rouchon, V.; Belhadj, O.; Duranton, M.; Gimat, A.; Massiani, P. Application of Arrhenius law to DP and zero-span tensile strength measurements taken on iron gall ink impregnated papers: Relevance of artificial aging protocols. *Appl. Phys. A Mater. Sci. Process* **2016**, *122*, 1–10. [CrossRef]
12. Teixeira, N.; Nabais, P.; de Freitas, V.; Lopes, J.A.; Melo, M.J. In-depth phenolic characterization of iron gall inks by deconstructing representative Iberian recipes. *Sci. Rep.* **2021**, *11*, 8811. [CrossRef]
13. Polyphenols in Art—Chemistry Hand in Hand with Conservation of Cultural Heritage. Available online: https://sites.fct.unl.pt/polifenois_em_arte/ (accessed on 30 June 2025).
14. Wagner, F.E.; Lerf, A. Mössbauer Spectroscopic Investigation of FeII and FeIII 3,4,5-Trihydroxybenzoates (Gallates)—Proposed Model Compounds for Iron-Gall Inks. *Z. Anorg Allg. Chemie.* **2015**, *641*, 2384–2391. [CrossRef]
15. Lerf, A.; Wagner, F.E. Model compounds of iron gall inks—A Mössbauer study. *Hyperfine Interact.* **2016**, *237*, 1–12. [CrossRef]
16. Díaz Hidalgo, R.J.; Córdoba, R.; Grigoryan, H.; Vieira, M.; Melo, M.J.; Nabais, P.; Otero, V.; Teixeira, N.; Fani, S.; Al-Abbady, H. The making of black inks in an Arabic treatise by al-Qalalūsī dated from the 13th c.: Reproduction and characterisation of iron-gall ink recipes. *Herit. Sci.* **2023**, *11*, 1–14. [CrossRef]
17. Melo, M.J.; Otero, V.; Nabais, P.; Teixeira, N.; Pina, F.; Casanova, C.; Fragoso, S.; Sequeira, S.O. Iron-Gall Inks: A review of their degradation mechanisms and conservation treatments. *Herit. Sci.* **2022**, *10*, 145. [CrossRef]
18. Espina, A.; Cañamares, M.V.; Jurašeková, Z.; Sanchez-Cortes, S. Analysis of Iron Complexes of Tannic Acid and Other Related Polyphenols as Revealed by Spectroscopic Techniques: Implications in the Identification and Characterization of Iron Gall Inks in Historical Manuscripts. *ACS Omega* **2022**, *7*, 27937–27949. [CrossRef]
19. Ferretti, A.; Sabatini, F.; Degano, I. A Model Iron Gall Ink: An In-Depth Study of of Aging Processes Involving Gallic Acid. *Molecules* **2022**, *27*, 8603. [CrossRef]
20. Caterino, S.; Caniola, I.M.; Pignitter, M.; Zoleo, A.; Crestini, C.; Sanchez-Cortés, S.; Sterflinger, K.; Cappa, F. A Systematic Multianalytical Approach in the Study of Iron–Polyphenolic Complexes in Iron-Gall Inks: Exploring the Potentialities of Raman and Electron Paramagnetic Resonance. *Inorg. Chem.* **2025**, *64*, 4802–4816. [CrossRef]
21. Van Gulik, R.; Kersten-Pampiglione, N.E. A closer look at iron gall ink burn. *Restaurator* **1994**, *15*, 173–187. [CrossRef]
22. Morenus, L.S. In Search of a Remedy: History of Treating Iron-Gall Ink at the Library of Congress. *Book Pap. Group Annu.* **2003**, *22*, 119–125.
23. Reissland, B. Conservation—Early Methods 1890–1960 [Internet]. Iron Gall Ink Website. 1997. Available online: https://irongallink.org/conservation-early-methods-1890-1960.html (accessed on 1 June 2025).
24. Reissland, B.; Scheper, K.; Fleischer, S. Phytate—Treatment [Internet]. Iron Gall Ink Website. 2007. Available online: https://irongallink.org/phytate-treatment.html (accessed on 1 June 2025).
25. Kolar, J.; Strlič, M.; Budnar, M.; Malešič, J.; Šelih, V.S.; Simčič, J. Stabilisation of corrosive iron gall inks. *Acta Chim. Slov.* **2003**, *50*, 763–770.
26. Botti, L.; Mantovani, O.; Ruggiero, D. Calcium Phytate in the Treatment of Corrosion Caused by Iron Gall Inks: Effects on Paper. *Restaurator* **2005**, *26*, 44–62. [CrossRef]
27. Henniges, U.; Reibke, R.; Banik, G.; Huhsmann, E.; Hähner, U.; Prohaska, T.; Potthast, A. Iron gall ink-induced corrosion of cellulose: Aging, degradation and stabilization. Part 2: Application on historic sample material. *Cellulose* **2008**, *15*, 861–870. [CrossRef]
28. Nunes, M.; Olival, F.; Mitchell, S.G.; Claro, A.; Ferreira, T. A holistic approach to understanding the iron-gall inks in the historical documents of the Portuguese Inquisition (1570–1790). *Micron* **2023**, *165*, 103396. [CrossRef]
29. Teixeira, N.; Avó, J.; Cruz, H.; Moniz, T.; Rangel, M.; de Freitas, V.; Lima, J.C.; Melo, M.J.; Pina, F. Impact of Fe^{3+}/Polyphenol Ratio in Iron-gall Ink on Superoxide Formation: Rationalizing Historic Recipes from a Kinetic Study. *ChemPhysChem* **2024**, *26*, e202400859. [CrossRef]
30. Kolar, J.; Možir, A.; Strlič, M.; Bruin, G.D.; Pihlar, B.; Steemers, T. Stabilisation of iron gall ink: Aqueous treatment with magnesium phytate. *e-Preserv. Sci.* **2007**, *4*, 19–24.
31. Völkel, L.; Prohaska, T.; Potthast, A. Combining phytate treatment and nanocellulose stabilization for mitigating iron gall ink damage in historic papers. *Herit. Sci.* **2020**, *8*, 1–15. [CrossRef]
32. Rouchon, V.; Desroches, M.; Duplat, V.; Letouzey, M.; Stordiau-Pallot, J. Methods of aqueous treatments: The last resort for badly damaged iron gall ink manuscripts. *J. Pap. IADA Rep.-Mitteilungen IADA* **2012**, *13*, 7–13. [CrossRef]
33. Poggi, G.; Giorgi, R.; Toccafondi, N.; Katzur, V.; Baglioni, P. Hydroxide nanoparticles for deacidification and concomitant inhibition of iron-gall ink corrosion of paper. *Langmuir* **2010**, *26*, 19084–19090. [CrossRef]
34. Baglioni, P.; Chelazzi, D.; Giorgi, R.; Poggi, G. Reply to 'A Note of Caution on the Use of Calcium Nanoparticle Dispersions as Deacidifying Agents'. *Stud. Conserv.* **2024**, *69*, 477–483. [CrossRef]

35. Poggi, G.; Carmen, M.; Marin, E.; Francisco, J.; Giorgi, R.; Baglioni, P. Calcium hydroxide nanoparticles in hydroalcoholic gelatin solutions (GeolNan) for the deacidification and strengthening of papers containing iron gall ink. *J. Cult. Herit.* **2016**, *18*, 250–257. [CrossRef]
36. Baglioni, P.; Carretti, E.; Chelazzi, D. Nanomaterials in art conservation. *Nat. Nanotechnol.* **2015**, *10*, 287–290. [CrossRef]
37. Sequeira, S.; Casanova, C.; Cabrita, E.J. Deacidification of paper using dispersions of $Ca(OH)_2$ nanoparticles in isopropanol. Study of efficiency. *J. Cult. Herit.* **2006**, *7*, 264–272. [CrossRef]
38. Malešič, J.; Kadivec, M.; Kunaver, M.; Skalar, T.; Cigić, I.K. Nano calcium carbonate versus nano calcium hydroxide in alcohols as a deacidification medium for lignocellulosic paper. *Herit. Sci.* **2019**, *7*, 1–14. [CrossRef]
39. Cremonesi, P. A Note of Caution on the Use of Calcium Nanoparticle Dispersions as Deacidifying Agents. *Stud. Conserv.* **2021**, *68*, 128–135. [CrossRef]
40. Lerf, A.; Wagner, F.E.; Dreher, M.; Espejo, T.; Pérez-Rodríguez, J.-L. Mössbauer study of iron gall inks on historical documents. *Herit. Sci.* **2021**, *9*, 49. [CrossRef]
41. Salvadó, N.; Butí, S.; Nicholson, J.; Emerich, H.; Labrador, A.; Pradell, T. Identification of reaction compounds in micrometric layers from gothic paintings using combined SR-XRD and SR-FTIR. *Talanta* **2009**, *79*, 419–428. [CrossRef]
42. Otero, V.; Vilarigues, M.; Carlyle, L.; Cotte, M.; De Nolf, W.; Melo, M.J. A little key to oxalate formation in oil paints: Protective patina or chemical reactor? *Photochem. Photobiol. Sci.* **2018**, *17*, 266–270. [CrossRef]
43. Danon, J.; Darbou, M.; Flieder, F.; Genand-Riondet, N.; Imbert, P.; Jehanno, G.; Roussel, Y. Mössbauer Study of Ferro-Gallic Inks from Manuscripts of the XIIth and the XVth Centuries. Available online: http://zenith.mast.br/MAST_DOC/TEXTUAL/JD.T.2.7.004/JD.T.2.7.004_d13.pdf (accessed on 1 June 2025).
44. Wagner, B.; Bulska, E.; Stahl, B.; Heck, M.; Ortner, H.M. Analysis of Fe valence states in iron-gall inks from XVIth century manuscripts by ^{57}Fe Mössbauer spectroscopy. *Anal. Chim. Acta* **2004**, *527*, 195–202. [CrossRef]
45. La Camera, D. Crystal Formations Within Iron Gall Ink: Observations and Analysis. *J. Am. Inst. Conserv.* **2007**, *46*, 153–174. [CrossRef]
46. Marín, E.; Sistach, M.C.; Jiménez, J.; Clemente, M.; Garcia, G.; García, J.F. Distribution of acidity and alkalinity on degraded manuscripts containing iron gall ink. *Restaurator* **2015**, *36*, 229–247. [CrossRef]
47. Dazem, C.L.F.; Amombo Noa, F.M.; Nenwa, J.; Öhrström, L. Natural and synthetic metal oxalates—A topology approach. *CrystEngComm* **2019**, *21*, 6156–6164. [CrossRef]
48. Pan, A.; Shi, C.; Zhao, C.; Du, J.; Zhou, Y.; He, L. Chemistry and Heritage Conservation: Calcium-Based Mineralized Hydrogel for the Adhesive Restoration of Historical Artifacts. *J. Chem. Educ.* **2024**, *101*, 5386–5394. [CrossRef]
49. Khaksar-Baghan, N.; Koochakzaei, A.; Hamzavi, Y. An overview of gel-based cleaning approaches for art conservation. *Herit. Sci.* **2024**, *12*, 248. [CrossRef]
50. Guilminot, E. The Use of Hydrogels in the Treatment of Metal Cultural Heritage Objects. *Gels* **2023**, *9*, 191. [CrossRef]
51. Baglioni, P.; Berti, D.; Bonini, M.; Carretti, E.; Dei, L.; Fratini, E.; Giorgi, R. Micelle, microemulsions, and gels for the conservation of cultural heritage. *Adv. Colloid Interface Sci.* **2014**, *205*, 361–371. [CrossRef]
52. Duquette, D.; Dumont, M.J. Comparative studies of chemical crosslinking reactions and applications of bio-based hydrogels. *Polym. Bull.* **2019**, *76*, 2683–2710. [CrossRef]
53. Lee, C.; Fiocco, G.; Vigani, B.; Recca, T.; Milanese, C.; Delledonne, C.; Licchelli, M.; Rossi, S.; Chung, Y.; Volpi, F.; et al. Chemically Crosslinked Alginate Hydrogel with Polyaziridine: Effects on Physicochemical Properties and Promising Applications. *ChemPlusChem* **2024**, *90*, e202400649. [CrossRef]
54. Gurikov, P.; Smirnova, I. Non-Conventional Methods for Gelation of Alginate. *Gels* **2018**, *4*, 14. [CrossRef]
55. Teixeira, N.; Mateus, N.; de Freitas, V.; Oliveira, J. Wine industry by-product: Full polyphenolic characterization of grape stalks. *Food Chem.* **2018**, *268*, 110–117. [CrossRef]